Deciphering the electron transfer mechanisms for biogas upgrading to biomethane within bioelectrochemical systems

Pau Batlle-Vilanova[a], Sebastià Puig[a]*, Rafael Gonzalez-Olmos[a,b], Anna Vilajeliu-Pons[a], M. Dolors Balaguer[a], Jesús Colprim[a]

[a]LEQUIA, Institute of the Environment, University of Girona. Campus Montilivi, E-17071 Girona, Catalonia, Spain.

[b]Chemical Engineering Department. IQS-School of Engineering, Ramon Llull University, Via Augusta 390, Barcelona 08017, Spain

Electronic supplementary information (ESI)

Summary

This supporting information material provides some extra information about the materials and methods and the results obtained in batch and continuous mode, as well as calculations on the CE losses, and a more detailed composition of the microbial community of the biocathode. Seven additional figures and one table are presented within this document, which was divided into five different sections.

Section S1. Schematic representation of the BES and the equipment.

Figure S1. Schematic representation of the BES design and the equipment used in the present study.

Section S2. Calculation of the cathode surface area.

Section S3. Operational conditions and start-up of the BES.

Figure S2. Mode of operation, cathode potential, and carbon source of the BES. Dashed lines at the beginning of each period indicate the day at which changes were applied.

Figure S3. Current demand of the biocathode during the start-up period.

Section S4. BES performance during batch test and continuous operation

Figure S4. Methane cumulated over time during batch tests 1, 6 and 13. Regression coefficient (r^2) and the continuous line correspond to the linear plot obtained.

Figure S5. Comparative analysis between the CE, current demand, pH and production rate obtained during batch tests.

Section S5. Microbial analyses

Figure S6. SEM image of the biocathode graphite surface.

Figure S7. Detailed results obtained for the pyrosequencing analyses of the biocathode microbial community.

Section S6. Calculation of the CE losses

Table S1. Calculation of the CCR_{SO4}^{2-}, CCR_{O2} and CE_{loss} of the BES.

Section S1. Schematic representation of the BES and the equipment.

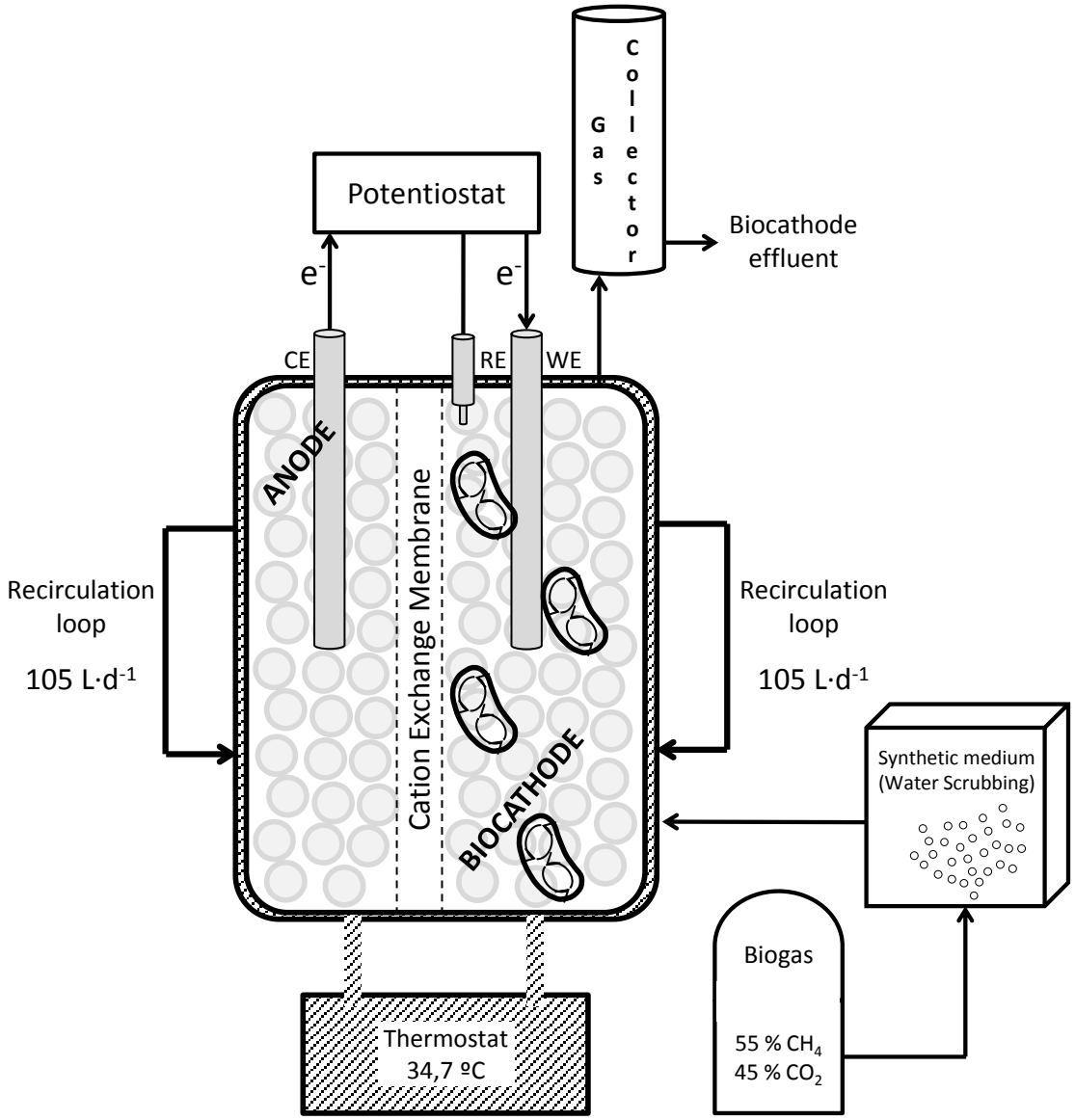

Figure S1. Schematic representation of the BES design and the equipment used in the present study.

Section S2. Calculation of the cathode surface area

To calculate the electrode surface of the cathode it was assumed that granular graphite was in form of spheres with a diameter of 4 mm (r=2mm).

The Area/m_{NCC}^3 ratio was calculated using the volume and area equations (equation and 2, respectively) of the sphere and using the net volume of the cathode chamber.

(1) $V = \frac{4}{3}\pi r^3$

(2) $A = 4\pi r^2$

Where, V is the volume of the sphere in m^3, A is the area in m^2, and r is the radius in m.

The volume of a sphere of granular graphite was $3.35 \cdot 10^{-8}$ m^3.

The number of spheres in the cathode can be subtracted from the ratio between the volume occupied by the spheres and the volume of each sphere.

The volume occupied by the spheres was $3.8 \cdot 10^{-4}$ m^3.

The number of spheres was 11340.

The area of a sphere of granular graphite was $5.03 \cdot 10^{-5}$ m^2.

The total area is obtained from multiplying the area of each sphere by the number of spheres. The total area was **0.57 m^2**.

Section S3. Operational conditions and start-up of the BES.

The BES was inoculated and started-up in continuous mode until an stable current demand and methane production were observed. Figure S1 show the diferent periods and the initial and end days for each of them. Figure S2 demonstrate the current demand of the biocathode during the start-up period (i.e. from day 0 to 159).

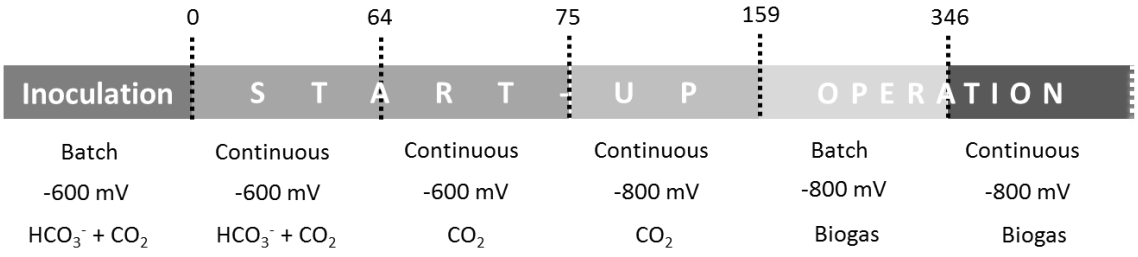

Figure S2. Mode of operation, cathode potential, and carbon source of the BES. Dashed lines at the beginning of each period indicate the day at which changes were applied.

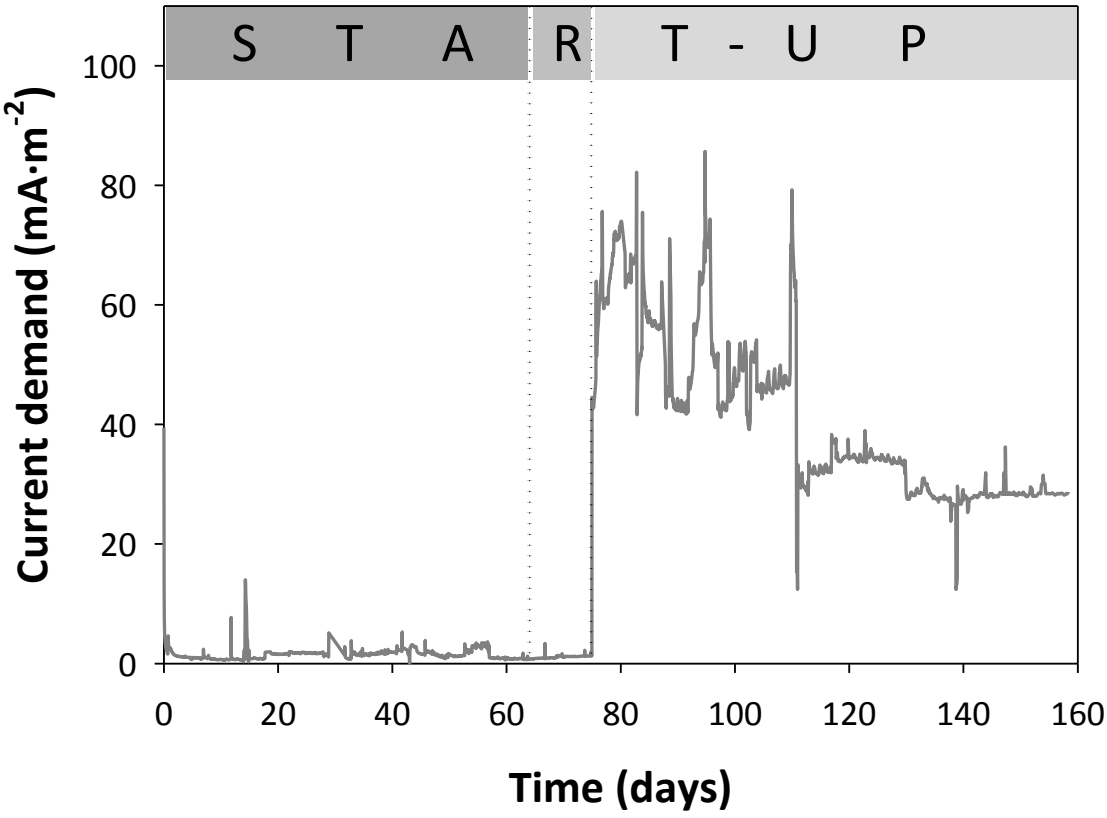

Figure S3. Current demand of the biocathode during the start-up period.

Section S4. BES performance during batch test and continuous operation

The amount of methane harvested over time in the most representative tests and the regression coefficient (r2) obtained for each plot are presented in figure S3. A comparative analysis of the different parameters of the system was performed to discern whether some parameters of the BES were related, and are shown in figure S4. It was found that there was not a direct relationship, except for the current demand and the production rate (r^2 = 0.990).

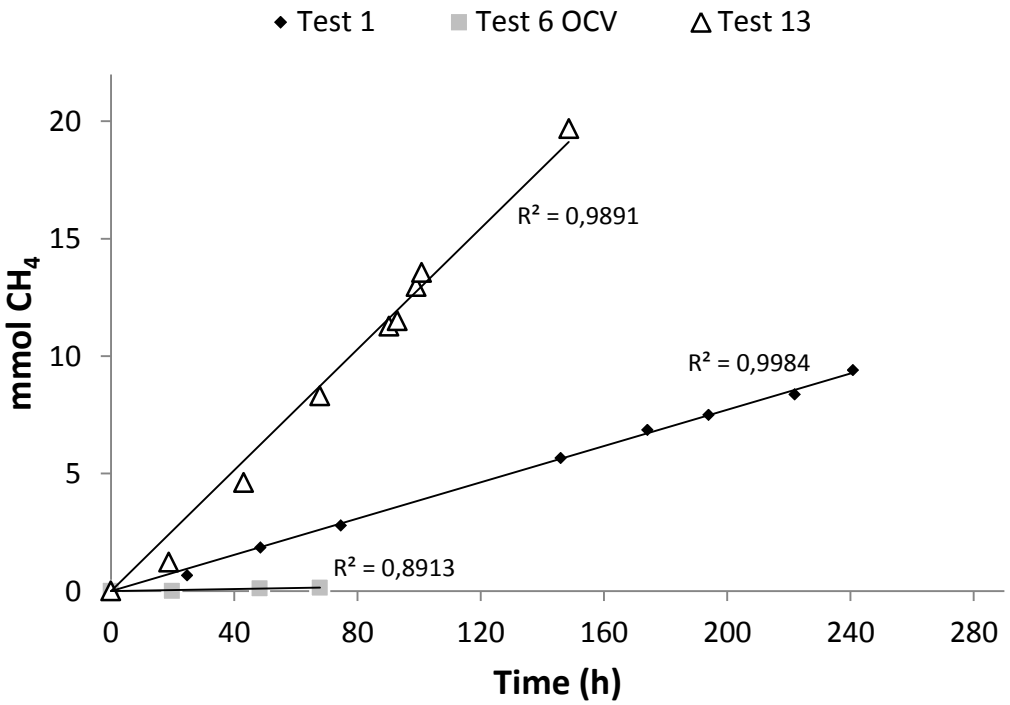

Figure S4. Methane cumulated over time during batch tests 1, 6 and 13. Regression coefficient (r^2) and the continuous line correspond to the linear plot obtained.

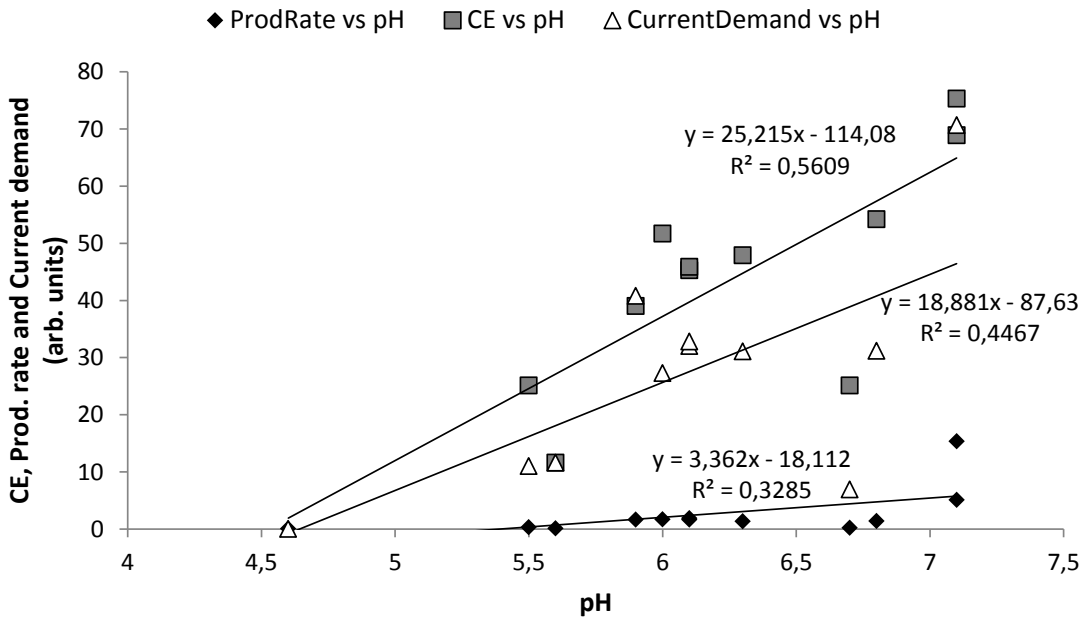

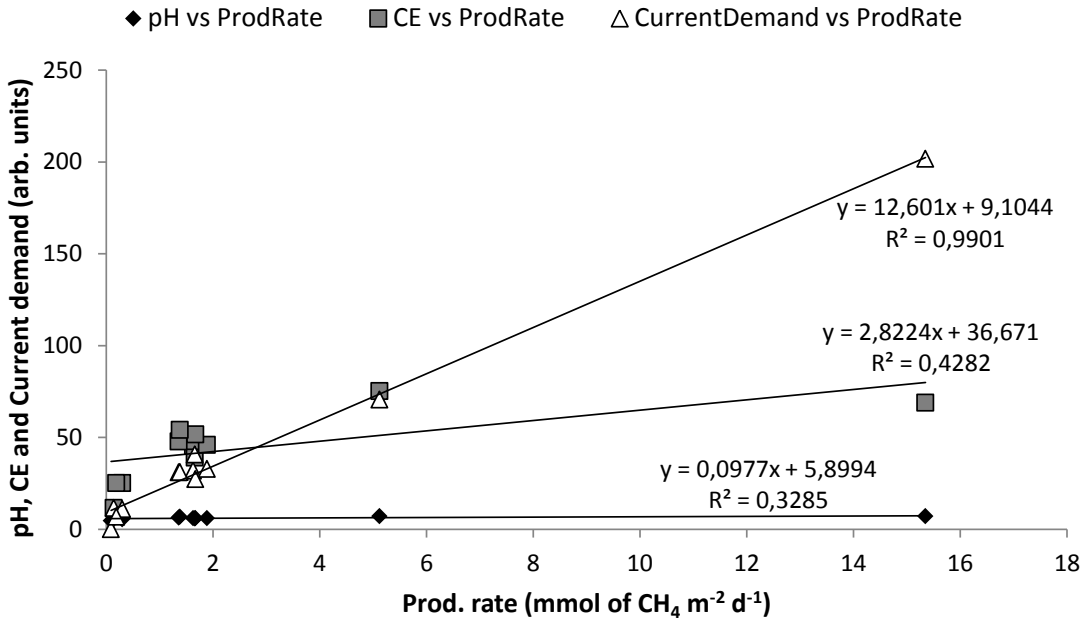

Figure S5a. Comparative analysis between the CE, current demand, pH and production rate obtained during batch tests.

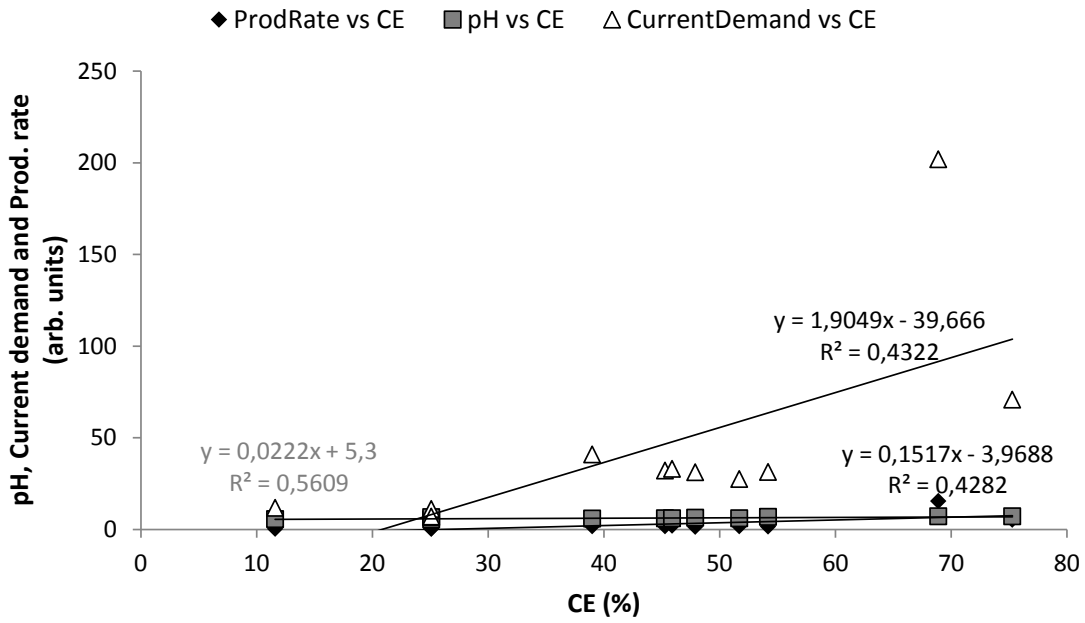

101

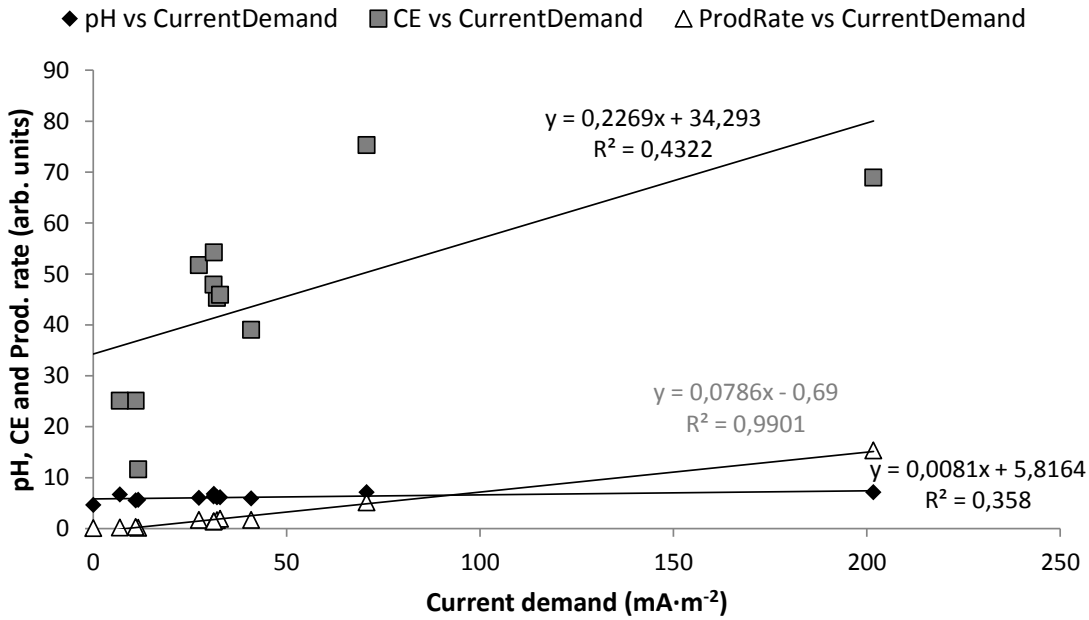

102

103 **Figure S5b**. Comparative analysis between the CE, current demand, pH and production

104 rate obtained during batch tests.

105

106

Section S5. Microbial analyses

Qualitative microbial analyses, such as scanning electron microscopy (SEM), were performed in graphite samples extracted from the biocathode. The materials and methods, and SEM images from the biocathode samples are shown in figure S5. The complete results from the pyrosequencing analyses of the microbial community of the biocathode are shown in high resolution in figure S6.

Scanning electron microscopy (SEM)

SEM analysis was performed at the same time as microbial community composition analysis (before starting test 3). Graphite samples from the biotic and abiotic MEC were extracted to compare the electrode surface. The samples were immersed in 2.5% (w/v) glutaraldehyde in a 0.1 M cacodylate buffer at pH 7.4 for a period of 4 hours. Next, the samples were washed and dehydrated in an ethanol series. Washes were done with cacodylate buffer and with water, both per duplicate. Dehydration with graded ethanol followed temperature steps of 50, 75, 80, 90, 95 and 3x100 ºC in periods of 20 minutes. The fixed samples were dried with a critical-point drier (model K-850 CPD, Emitech, Alemanya) and sputtered-coated with a 40 nm gold layer. The coated samples were examined with a SEM (model DSM-960; Zeiss, Germany) at 20 kV and images were captured digitally. Energy-dispersive X-ray spectroscopy (EDX; QUANTAX Microanalysis System) was also performed in the abiotic MEC graphite samples in order to identify the compounds deposited on the surface. Analyzed samples were not pretreated. Digital images of both SEM and EDX analysis were collected and processed by ESPRIT 1.9 BRUKER program (AXS Microanalysis GmbH, Berlin, Germany).

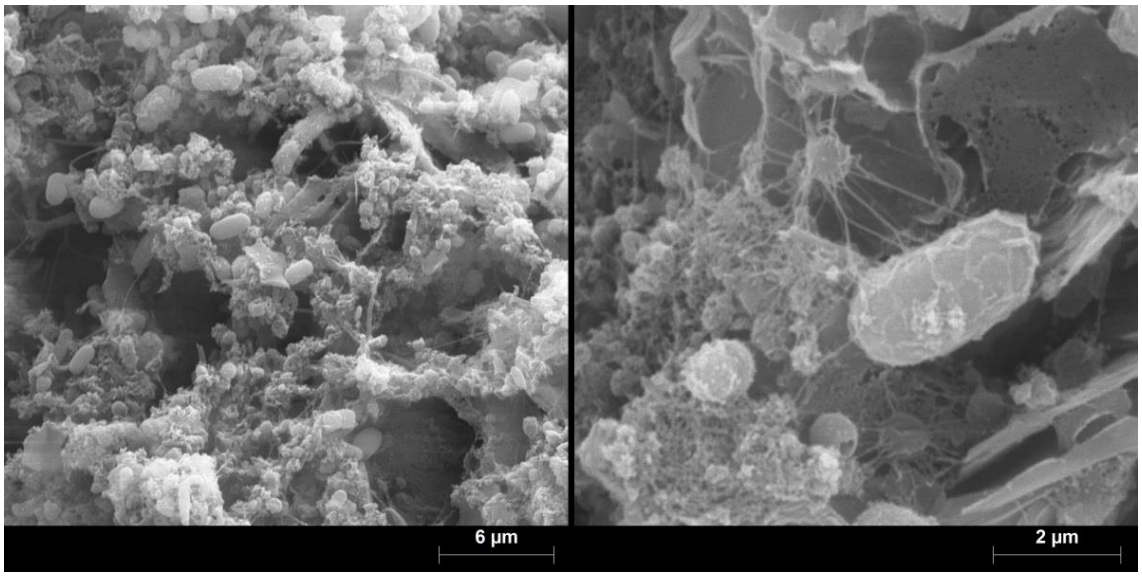

Figure S6. Scannning electron microscopy (SEM) image of the biocathode graphite surface.

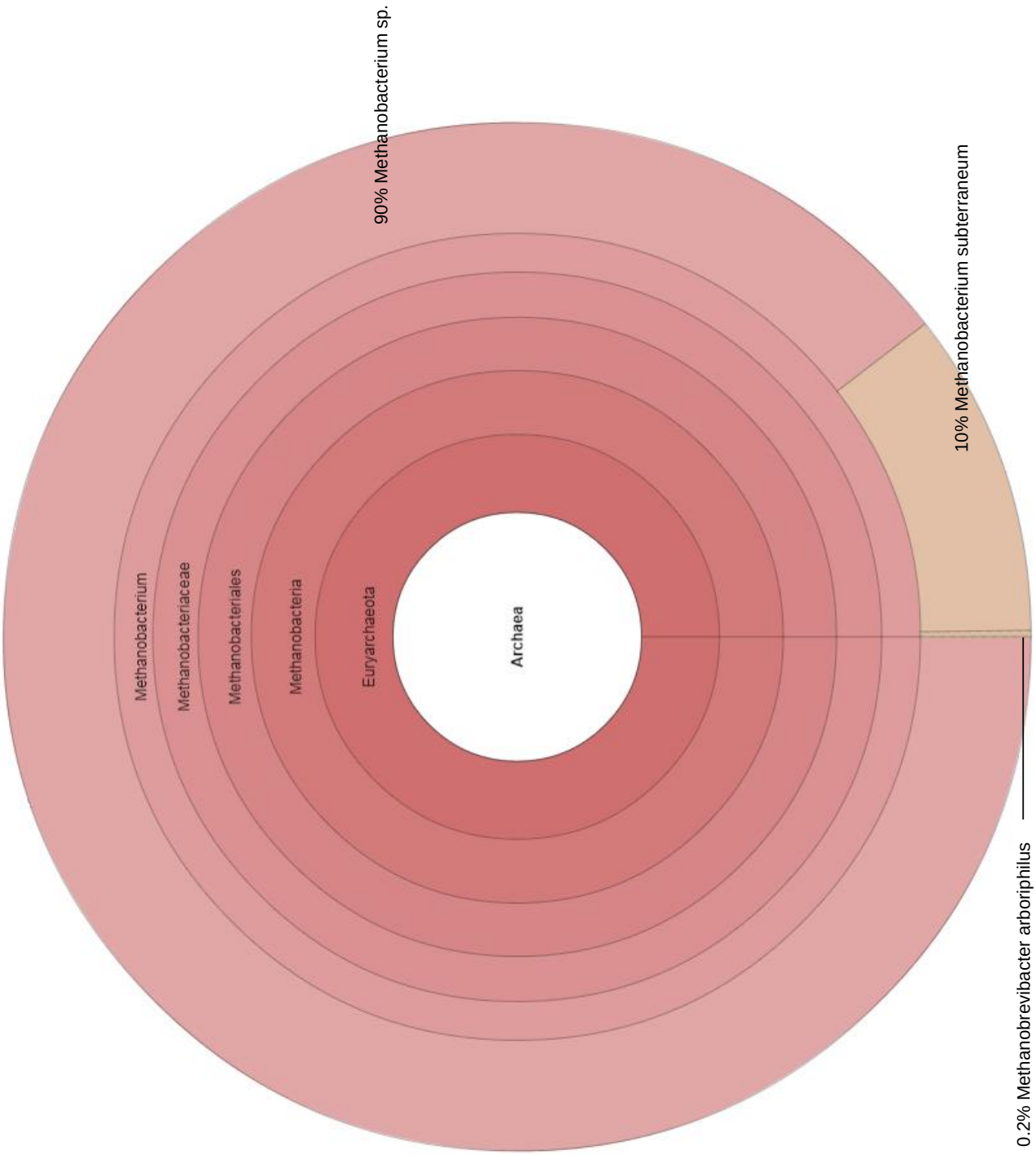

137

138 **Figure S7a.** Detailed results obtained for the pyrosequencing analyses of the
139 biocathode microbial community.

140

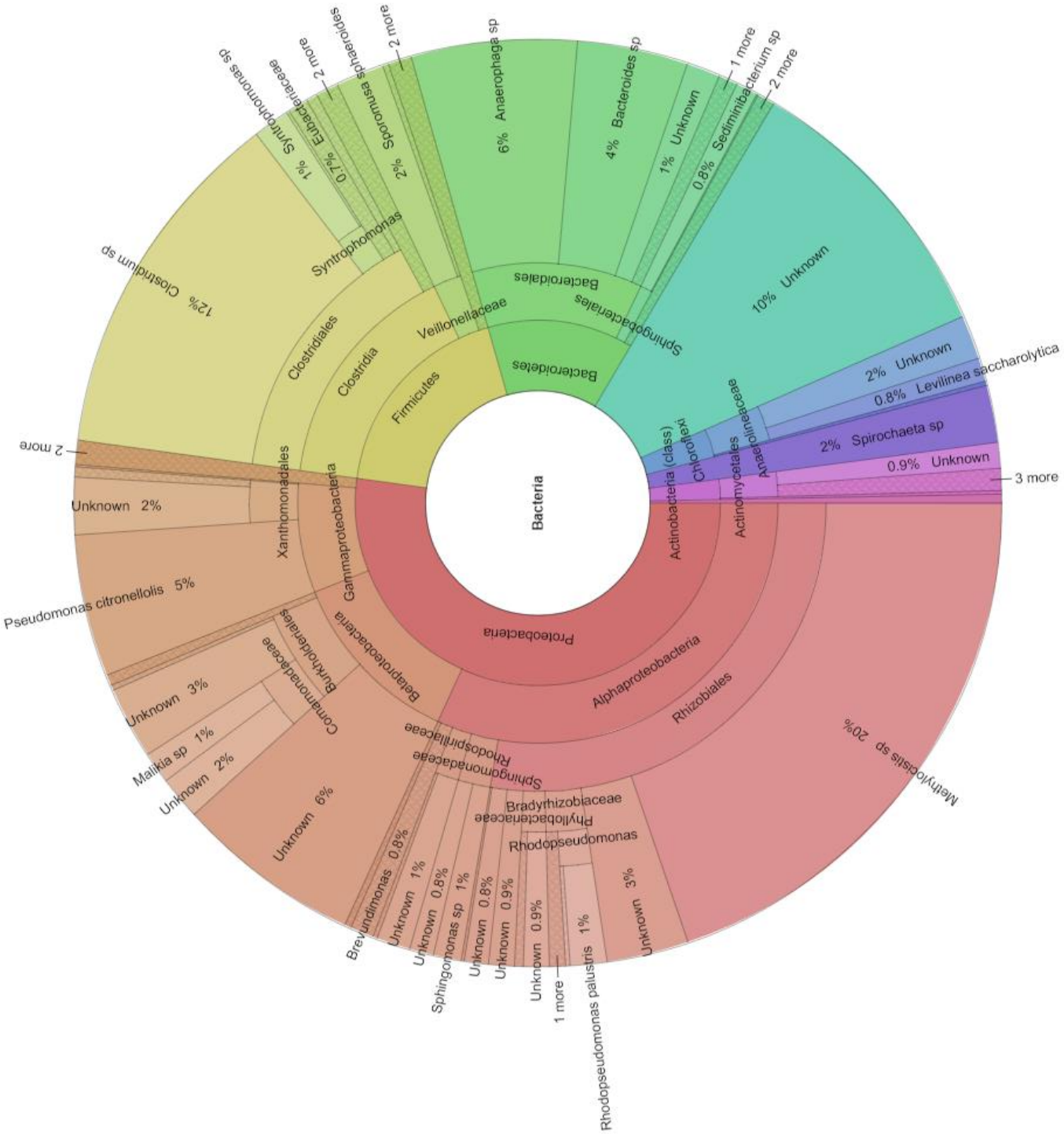

141

142 **Figure S7b.** Detailed results obtained for the pyrosequencing analyses of the
143 biocathode microbial community.

144

Section S6. Calculation of the CE losses

The coulombs consumed by cross-over reactions were quantified from the oxygen diffusion and the sulphate reduction in the biocathode, and compared to the Coulombs consumed for methane production to estimate the CE losses according to equation 3.

(3) $\mathrm{CE_{loss}}(\%) = 100 \cdot (\mathrm{CCR_{O2}} + \mathrm{CCR_{SO4^{2-}}})/\mathrm{CRR}$

Where CCR is the coulombic consumption rate obtained from the coulombs consumed over time, CCR_{O2} is the coulombic consumption rate due to oxygen oxidation and CCR_{SO4}^{2-} is the coulombic consumption rate due to sulphate reduction.

CCR, CCR_{SO4}^{2-} and CCR_{O2} are expressed in Coulombs d^{-1}. CCR_{CH4} and CCR_{SO4}^{2-} were calculated according to equation 4 and 5, respectively:

(4) $\mathrm{CCR_{CH4}} = 8 \cdot \mathrm{m_{CH4}} \cdot \mathrm{F}$

(5) $\mathrm{CCR_{SO4^{2-}}} = 8 \cdot \mathrm{m_{SO4^{2-}}} \cdot \mathrm{F}$

In equation 2, m_{CH4} is the slope of the linear plot obtained from the moles of methane harvested over time (moles d^{-1}), 8 are the number of electrons consumed per mole of methane produced, and F is Faraday's constant (96485 C mole of electrons^{-1}). In equation 3, m_{SO4}^{2-} is the slope corresponding to the sulphate consumption rate (moles d^{-1}), and 8 are the number of electron consumed to reduce one mole of sulphate to hydrogen sulphide, according to equation 6.

(6) $\mathrm{SO_4^{2-}} + 10\mathrm{H^+} + 8\mathrm{e^-} \rightarrow \mathrm{H_2S} + \mathrm{H_2O}$

Once in the cathode chamber, oxygen can be electrochemically reduced according to Equation 7, or used to biologically oxidize methane by *Methylocystis* sp. according to Equation 8.

(7) $\mathrm{O_2} + 2\mathrm{H^+} + 2\mathrm{e^-} \rightarrow \mathrm{H_2O}$

(8) $\mathrm{CH_4} + 2\mathrm{O_2} \rightarrow \mathrm{CO_2} + \mathrm{H_2O}$

Therefore, CCR_{O2} can be calculated by two different equations, one considering directly O_2 reduction (equation 9) and the other considering the methane consumed (equation 10).

(9) $\mathrm{CCR_{O2}} = \mathrm{J_{O2}} \cdot \mathrm{A} \cdot 2 \cdot \mathrm{F}$

(10) $$\mathrm{CCR_{O2}} = \frac{\mathrm{J_{O2}} \cdot \mathrm{A} \cdot 8 \cdot \mathrm{F}}{2}$$

Where in equation 9, J_{O2} is the oxygen diffusion flux (mol_{O2} m^{-2} d^{-1}), A is the membrane area (0,04 m^2), 2 is the moles of electron that are electrochemically consumed per

178 mole of oxygen, and F is Faraday's constant. In equation 10, 8 correspond to the moles
179 of electrons consumed per mole of methane produced, and 2 to the number of moles
180 of oxygen necessary to oxidize 1 mole of methane (equation 8).

181 Oxygen diffusion flux (J_{O2}) was calculated according to other authors,[1] from Equation
182 11.

183 (11) $$J_{O2} = \frac{D_{O2} \cdot (C_{O2,an} - C_{o2,cat})}{\delta}$$

184 Where D_{O2} is the is the diffusion coefficient of oxygen determined for a CMI-7000
185 cation exchange membrane (Membrane International Inc.,USA) ($3.72 \cdot 10^{-5}$ m^2 d^{-1}).[2]
186 $C_{O2,an}$ and $C_{O2,cat}$ are the dissolved oxygen concentration in the anode and cathode
187 compartments (mole O_2 m^{-3}), respectively; and δ the thickness of the membrane
188 ($0.45 \cdot 10^{-3}$ m). The resulting units for oxygen diffusion flux are mole O_2 m^{-2} d^{-1}.

189

Table S1. Calculation of the CCR_{SO4}^{2-}, CCR_{O2} and CE_{loss} of the BES.

Test	CE (%)	CRR (C d^{-1})	CCR_{SO4}^{2-} (C d^{-1})	CCR_{O2} Eq. 7 (C d^{-1})	CCR_{O2} Eq. 8 (C d^{-1})	CE_{loss} (%)
1	45.3 ± 1.9	1583.1	1.8	178.9	356.8	11.3 - 22.5
2	39.0 ± 1.6	1877.8	1.8	178.9	356.8	9.5 - 19.0
3	47.9 ± 5.8	1265.1	1.8	178.9	356.8	14.1 - 28.2
4	45.9 ± 3.6	1818.1	1.8	178.9	356.8	9.8 - 19.6
5	51.7 ± 4.5	1425.4	1.8	178.9	356.8	12.5 - 25.0
6	n/a	n/a	n/a	n/a	n/a	n/a
7	11.6 ± 0.9	533.3	1.8	178.9	356.8	33.5 - 66.9
8	25.1 ± 4.7	541.0	1.8	178.9	356.8	33.1 - 66.0
9	25.1 ± 2.3	342.5	1.8	178.9	356.8	52.2 - 104.2
10	n/a	n/a	n/a	n/a	n/a	n/a
11	n/a	n/a	n/a	n/a	n/a	n/a
12	54.2 ± 8.3	1330.2	1.8	178.9	356.8	13.4 - 26.8
13	75.3 ± 5.2	3133.3	1.8	178.9	356.8	5.7 - 11.4
14	68.9 ± 0.8	6390.8	23.2	178.9	356.8	3.2 - 5.6

190

191 In all cases, the major contributor to the CE losses was the oxygen that diffused from
192 the anode to the cathode. The presence of *Methylocystis* sp. caused the CE of the BES
193 to be lower than it would be considering only pure electrochemical O_2 reduction.

(1) Van Eerten-jansen, M. C. A. A.; Ter Heijne, A.; Buisman, C. J. N.; Hamelers, H. V. M. Microbial electrolysis cells for production of methane from CO2: long-term performance and perspectives. *Int. J. Energy Res.* **2012**, 809–819.

(2) Kim, J. R.; Cheng, S.; Oh, S.-E.; Logan, B. E. Power generation using different cation, anion, and ultrafiltration membranes in microbial fuel cells. *Environ. Sci. Technol.* **2007**, *41*, 1004–1009.